UNIVERSIDADE FEDERAL DO RIO GRANDE DO SUL
FACULDADE DE ODONTOLOGIA
LABORATÓRIO DE MATERIAIS DENTÁRIOS

EDUARDO ANTUNES DA CUNHA BAHLIS

DESENVOLVIMENTO DE MEMBRANA REABSORVÍVEL DE PBAT/BAGNb PARA REGENERAÇÃO ÓSSEA GUIADA

Porto Alegre
2021

EDUARDO ANTUNES DA CUNHA BAHLIS

DESENVOLVIMENTO DE MEMBRANA REABSORVÍVEL DE PBAT/BAGNb PARA REGENERAÇÃO ÓSSEA GUIADA

Trabalho de conclusão de curso de graduação apresentado à Faculdade de Odontologia da Universidade Federal do Rio Grande do Sul como requisito obrigatório para a obtenção do título de cirurgião-dentista.

Orientador: Prof. Dr. Vicente Castelo Branco Leitune

Porto Alegre

2021

À minha mãe, a mulher mais corajosa que já conheci.

AGRADECIMENTOS

Agradeço,

Aos professores Vicente e Fabrício, e à doutoranda Gabriela, pelo conhecimento compartilhado nos últimos anos e pela grande contribuição com meu desenvolvimento profissional.

À minha mãe, Angela, por me ensinar valores e princípios, e por enfrentar todos os obstáculos necessários para me ver feliz.

Ao meu padrasto, Julio, por me acolher como filho e por tornar essa conquista possível, e aos demais familiares pelo apoio e suporte oferecido.

À minha namorada, Liliana, pelo companheirismo, carinho e apoio nas mais diversas situações.

Aos amigos de longa data, pela amizade leal e verdadeira ao longo do tempo.

Aos amigos e colegas de faculdade, pela grande amizade construída ao longo da graduação e que perdurará.

Um agradecimento especial àquele que torceu veementemente por essa conquista, mas que hoje a observa das estrelas. Obrigado, pai.

RESUMO

O objetivo deste estudo foi desenvolver uma membrana compósita reabsorvível de poli(butileno adipato co-tereftalato) (PBAT) e vidro bioativo contendo nióbio (BAGNb) para aplicação em regeneração óssea guiada (ROG). As membranas foram produzidas por evaporação de solvente com diferentes concentrações de BAGNb (10%, 20% e 30%) e caracterizadas por diferentes métodos. Foi produzida uma membrana sem adição de BAGNb, como controle. A análise das ligações químicas dos materiais foi realizada através da espectroscopia de infravermelho (FTIR-ATR) (n=1). As imagens das membranas foram obtidas por meio da microscopia eletrônica de varredura, onde as amostras foram avaliadas em um microscópio eletrônico (Jeol 6060) em magnificação de 100, 1.000 e 10.000x (n=1). O teste termogravimétrico foi realizado para avaliar a degradação das membranas in vitro após diferentes tempos de imersão em SBF (TGA) (n=1). O ângulo de contato foi avaliado em um tensiômetro pelo método de gota séssil utilizando água (n=3). A rugosidade das superfícies das membranas foi avaliada através da perfilometria (n=3) e o pH foi medido em pHmetro digital utilizando água destilada nos tempos inicial, 1h, 2h, 4h, 24h, 72h, 7d, 14d, 21d e 28d (n=1). As propriedades mecânicas das membranas foram avaliadas em máquina de ensaio de acordo com a ASTM D638. Células MC3T3-E1 foram utilizadas para a análise da viabilidade celular por SRB e mineralização celular por Alizarin S Red. Na análise por FTIR, foram observadas ligações Si-O-Si (1050cm^{-1} e 450cm^{-1}) C=O (1700cm^{-1}) e C-H(1105cm^{-1}, 1270cm^{-1}, 2960cm^{-1}). A microscopia eletrônica de varredura revelou partículas de biovidro na superfície das membranas dos grupos teste. O aumento da concentração de BAGNb reduziu a temperatura para degradação das membranas no teste de termogravimetria (TGA). A adição de BAGNb à membrana reduziu o ângulo de contato do material em relação ao grupo controle e a adição de 30% aumentou a rugosidade das amostras, atingindo média de 1,43µm. Foi observado aumento do pH após 24 horas em água destilada. Com o aumento da concentração de BAGNb, houve redução da resistência e da % de alongamento e aumento do módulo de elasticidade dos materiais. Houve aumento da viabilidade celular e da mineralização com a adição de BAGNb. Após 14 dias de cultura a % de área mineralizada variou entre 0,98% e 4,78%. A adição de BAGNb ao PBAT resultou em membranas com propriedades satisfatórias e potencial de remineralização para a aplicação técnicas de regeneração óssea guiada.

Palavras chave: Regeneração óssea. Biomateriais. Nióbio.

ABSTRACT

The aim of present study was to develop a polybutylene-adipate-terephthalate and niobium-containing bioactive glasses resorbable membrane for guided bone regeneration (GBR). Barrier membranes were manufactured by solvent casting with different concentrations of BAGNb (10, 20 and 30%) and characterized by different methods. Membranes without addition of BAGNb were produced as control. Fourier-transformed infrared spectroscopy (FTIR-ATR) was performed to analyze the chemistry structure of composites (n=1). The morphology of the membrane's surfaces was evaluated by scanning electron microscopy (SEM) using a electron microscope (Jeol 6060) in 500x magnification (n=1). Termogravimetry (TGA) was performed to assess the in vitro thermal behavior after immersion in SBF. The contact angle was evaluated in a optical tensiometer by sessil drop method using distilled water (n=3). The surface roughness of the membranes was assessed through optical perfilometry (n=3). Membrane samples were immersed in deionized water and pH was measured for up to 28 days using a digital pHmeter. The mechanical behavior of developed membranes was evaluated by a tensile test with specimens that were prepared according to ASTM D638–02. MC3T3-E1 cells were used for SRB and Alizarin S Red analysis. In the FTIR analysis, Si-O-Si, C=O and C-H bonding were observed. SEM analysis revealed bioactive glass particles on the surface of the membranes. The increase of concentration of BAGNb influenced the thermal behavior of the membranes in termogravimetry analysis. The addition of BAGNb decreased the contact angle compared to control group. At 30% group, there was increased of roughness, reaching a mean 1,43µm. The pH values increased after 24h. The addition of BAGNb reduced the tensile strength and elongation rate, and increased the Young's module. There was increased of the cell viability and mineralization with addition of BAGNb. After 14 days of culture, the % of mineralized area ranged between 0.98% and 4.78%. The addition of BAGNb in PBAT produced membranes with satisfactory properties and remineralization potential for applying in GBR techniques.

Keywords: Bone regeneration. Biomaterial. Niobium.

SUMÁRIO

1 INTRODUÇÃO

O alvéolo dentário é remodelado por uma série de eventos fisiológicos após a extração dentária. Estes eventos geram alterações dimensionais relevantes, como redução horizontal e vertical, principalmente na região vestibular (ARAÚJO; LINDHE, 2005; CARDAROPOLI; ARAÚJO; LINDHE, 2003; COUSO-QUEIRUGA *et al.*, 2021; MISAWA; LINDHE; ARAÚJO, 2016). A atrofia alveolar pode acarretar em tecido ósseo de suporte insuficiente para a instalação de implantes dentários, dificultando o planejamento e a execução do tratamento reabilitador, e a utilização de enxertos pode ser necessária para viabilizar a instalação dos implantes (AVILA-ORTIZ, Gustavo; CHAMBRONE; VIGNOLETTI, 2019). A regeneração óssea guiada (ROG) preconiza a utilização de membranas como barreira para compartimentalizar o defeito ósseo e impedir a invaginação de tecido conjuntivo e epitelial na intenção de favorecer o povoamento de células específicas, reduzir a taxa de reabsorção e a magnitude das alterações dimensionais causadas por esta (ELGALI *et al.*, 2017; RETZEPI; DONOS, 2010). Diferentes procedimentos odontológicos utilizam os princípios da ROG, como aumento ósseo vertical e horizontal (CUCCHI *et al.*, 2019; MENDOZA-AZPUR *et al.*, 2019), preservação óssea alveolar (AVILA-ORTIZ, G. *et al.*, 2020; CHA *et al.*, 2019; TONETTI *et al.*, 2019) e tratamento de defeitos circundantes ao implante dentário (CLEMENTINI *et al.*, 2019; TEMMERMAN *et al.*, 2020). Um dos principais componentes da ROG e destes procedimentos é a membrana utilizada como barreira. Idealmente, estas membranas devem oferecer resistência mecânica, fácil manipulação, biocompatibilidade, tempo de degradação adequado e absorvibilidade (CABALLÉ-SERRANO *et al.*, 2018; RAKHMATIA *et al.*, 2013)

As membranas utilizadas podem ser não reabsorvíveis ou reabsorvíveis. As membranas não reabsorvíveis, como as de titânio e poli(tetrafluoretileno) (PTFE) são utilizadas e exercem função passiva, protegendo o defeito alveolar. Contudo, a resistência à reabsorção implica a necessidade de intervenção cirúrgica adicional para a remoção da membrana (ATEF *et al.*, 2020; NAENNI *et al.*, 2017). Atualmente, as membranas reabsorvíveis são produzidas a fim de reduzir o número de intervenções e a morbidade do paciente e estimular o

processo de regeneração, não só protegendo o defeito, mas participando ativamente da cicatrização (HAGHIGHAT *et al.*, 2019; PITALUGA *et al.*, 2018; SU *et al.*, 2021). Grande parte das membranas reabsorvíveis comercialmente disponíveis são compostas por colágeno e apresentam algumas características indesejáveis, como dificuldade de manuseio, baixa resistência mecânica, taxa de degradação irregular e aumento da penetração bacteriana alveolar (BUNYARATAVEJ; WANG, 2001; CABALLÉ-SERRANO *et al.*, 2018; VON ARX *et al.*, 2005). Como alternativa, são desenvolvidas membranas reabsorvíveis compósitas que compreendem materiais poliméricos e cerâmicos com o objetivo de aprimorar as propriedades do material.

Alguns dos polímeros sintéticos reabsorvíveis estudados para a produção de membranas compósitas são o Poli(L-ácido láctico) (PLLA) (BYEON *et al.*, 2013), o poli(ácido lático-coácido glicólico) (PLGA) (YOSHIMOTO *et al.*, 2018) e Policaprolactona (PCL) (ALLO; RIZKALLA; MEQUANINT, 2010). O poli(butileno adipato co-tereftalato) (PBAT) é um polímero reabsorvível que apresenta características promissoras para a aplicação em membranas para regeneração óssea por ser mais flexível quando comparado aos outros polímeros já utilizados(FUKUSHIMA *et al.*, 2012; MALLEGNI *et al.*, 2018; WEI *et al.*, 2016), o que pode facilitar a manipulação da membrana e sua adaptação nas margens da ferida. Além disso, oferece boas propriedades térmicas, biodegradação, biocompatibilidade e capacidade de suportar a proliferação celular (ARSLAN *et al.*, 2016). Com a finalidade de aprimorar e modificar as propriedades das membranas, materiais cerâmicos são utilizados em conjunto ao polímero. Dessa forma, a incorporação de partículas cerâmicas à matriz polimérica possibilita a produção de um material com boas propriedades mecânicas e capaz de estimular processos regenerativos (SUNANDHAKUMARI *et al.*, 2018; YUSOF *et al.*, 2019).

Considerando os materiais cerâmicos disponíveis para produção das membranas, o vidro bioativo possui a capacidade de estimular a deposição de tecido ósseo, regular a atividade e induzir a mudança de fase do ciclo celular, aumentando a expressão de genes envolvidos no processo de ossificação (HENCH, 2006; JONES, 2015; XYNOS *et al.*, 2000). Além disso, oferece a

possibilidade de incorporação de íons metálicos adjuvantes com o intuito de otimizar as propriedades osteogênica, angiogênica e antibacteriana (GU *et al.*, 2014; LIN *et al.*, 2016; OH; WON; KIM, 2012). O nióbio é um metal biocompatível e já vem sendo utilizado em aplicações biomédicas (ALTMANN *et al.*, 2017; BALBINOT *et al.*, 2020; LEITUNE *et al.*, 2013). Quando adicionado aos vidros bioativos, o nióbio demonstrou capacidade de estimular a produção mineral in vitro, aumentando taxas de mineralização celular, e in vivo, induzindo a formação óssea em defeitos críticos em modelo animal (BALBINOT *et al.*, 2018, 2019; DSOUKI *et al.*, 2014).

Procura-se desenvolver novas membranas que apresentem os requisitos exigidos para o uso em procedimentos de ROG e que preencham as lacunas deixadas pelos materiais disponíveis atualmente. Apesar das desvantagens apresentadas pelas membranas existentes e das adequadas propriedades do PBAT, a literatura ainda não descreve sua utilização em membranas para ROG, bem como a união entre o polímero e o vidro bioativo contendo nióbio.

2 OBJETIVOS

O objetivo deste estudo foi desenvolver uma membrana reabsorvível de PBAT/BAGNb para regeneração óssea guiada.

3 ARTIGO CIENTÍFICO

Este trabalho de conclusão de curso apresenta-se na forma de artigo científico, escrito na língua inglesa e segue as normas referentes ao periódico Materials Science and Engineering C (ISSN: 0928-4931), no qual está publicado. https://doi.org/10.1016/j.msec.2021.112115

Polybutylene-adipate-terephthalate and niobium-containing bioactive glasses composites: development of barrier membranes with adjusted properties for guided bone regeneration.

Abbreviated Title: PBAT/BAGNb barrier membranes for GBR.

Gabriela de Souza Balbinot, DDS, MSc, PhD student - Dental Materials Laboratory, School of Dentistry. Universidade Federal do Rio Grande do Sul, Porto Alegre, RS, Brazil. gabriela.balbinot@ufrgs.br ORCID: 0000-0001-9076-2460

Eduardo Antunes da Cunha Bahlis, Undergraduate Student - Dental Materials Laboratory, School of Dentistry. Universidade Federal do Rio Grande do Sul, Porto Alegre, RS, Brazil eduardo.bahlis@ufrgs.br ORCID: 0000-0001-7457-6094

Fernanda Visioli, DDS, MSc, PhD, Adjunct Professor - Patology Laboratory, School of Dentistry. Universidade Federal do Rio Grande do Sul, Porto Alegre, RS, Brazil. fernanda.visioli@ufrgs.br ORCID: 0000-0002-4033-8431

Vicente Castelo Branco Leitune, DDS, MSc, PhD, Adjunct Professor - Dental Materials Laboratory, School of Dentistry. Universidade Federal do Rio Grande do Sul, Porto Alegre, RS, Brazil. vicente.leitune@ufrgs.br ORCID: 0000-0002-5415-1731

Rosane Michele Duarte Soares, MSc, PhD, Associate Professor - Chemestry Institute, Universidade Federal do Rio Grande do Sul. Porto Alegre, Rio Grande do Sul, Brazil. soaresr@ufrgs.br ORCID: 0000-0002-5225-7559

Fabricio Mezzomo Collares, DDS, MSc, PhD, Adjunct Professor - Dental Materials Laboratory, School of Dentistry. Universidade Federal do Rio Grande do Sul, Porto Alegre, RS, Brazil. fabricio.collares@ufrgs. ORCID: 0000-0002-1382-0150

Corresponding Author

Fabricio Mezzomo Collares

+555133085198. fabricio.collares@ufrgs.br

Rua Ramiro Barcelos, 2492. Porto Alegre, Rio Grande do Sul. Brazil.

Author Contributions

Gabriela de Souza Balbinot: Conceptualization, Investigation, Formal Analysis, Data curation, Project Administration, Writing -Original Draft. **Eduardo Antunes da Cunha Bahlis**: Investigation, Data curation. **Fernanda Visioli**: Methodology, Resources, Founding Acquisition. **Vicente Castelo Branco Leitune**: Conceptualization, Methodology, Writing - Review & Editing, Founding Acquisition. **Rosane Michele Duarte Soares**: Methodology, Writing - Review & Editing, Founding Acquisition. **Fabricio Mezzomo Collares**: Conceptualization, Methodology, Writing - Review & Editing, Founding Acquisition, Supervision.

Funding

This study was partially financed by CNPq “Conselho Nacional de Desenvolvimento Científico e Tecnológico” (308196/2019-8).

Acknowledgments

G.S.B would like to thank CAPES "Coordenação de Aperfeiçoamento de Pessoal de Nível Superior - Brasil - Finance Code 001" and E.A.C.B would like to thank CNPq “Conselho Nacional de Desenvolvimento Científico e Tecnológico” for scholarship. The authors gratefully acknowledge the CBMM (Companhia Brasileira de Metalurgia e Mineração) for providing the Niobium Chloride used in this study.

Abstract

This study aimed to develop bioactive guided bone regeneration (GBR) membranes by manufacturing PBAT/BAGNb composites as casting films. Composites were produced by melt-extrusion, and BAGNb was added at 10wt%, 20wt%, and 30wt% concentration. Pure PBAT membranes were used as a control (0wt%BAGNb). FTIR and thermogravimetric analysis characterized the composites. Barrier membranes were produced by solvent casting, and their mechanical and surface properties were assessed by tensile strength test and contact angle analysis, respectively. The ion release and cell behavior were evaluated by pH, cell proliferation, and mineralization. Composites were successfully produced, and the chemical structure showed no interference of BAGNb in the PBAT structure. The addition of BAGNb increased the stiffness of the membranes and reduced the contact angle, increasing the roughness in one side of the membrane. Sustained pH increment was observed for BAGNb-containing membranes with increased proliferation and mineralization as the concentration of BAGNb increases. The incorporation of up to 30wt% of BAGNb into PBAT barrier membranes was able to maintain adequate chemical-mechanical properties leading to the production of materials with tailored surface properties and bioactivity. Finally, this biomaterial class showed outstanding potential and may contribute to bone formation in GBR procedures.

Keywords: Regenerative Medicine, Guided Tissue Regeneration, Alveolar Ridge Augmentation, Biopolymer, Niobium.

The functional and aesthetic reconstruction in bone tissue is frequently needed for dental implant procedures in craniofacial surgery [1,2]. Guided bone regeneration (GBR) has been used as a strategy to achieve lateral and vertical bone augmentation by creating and maintaining space for bone regeneration [3]. This technique is frequently applied for alveolar bone maintenance [4] and relies on the application of barrier membranes to protect the bone defect allowing osteogenesis without the ingrowth and proliferation of epithelial and connective tissue cells into the defect, which could impair an adequate newly bone formation [5–7]. These procedures' success is related to the stability of the membrane and the ability of bone growth in the maintained space [3,4,8].

The space maintenance capacity differs considering a wide range of properties that are observed in GBR membranes. Among commercially available materials, polytetrafluoroethylene (PTFE), titanium meshes, collagen membranes, and synthetic polyesters are used for this purpose, and the variable properties of these two materials are related to some drawbacks in these treatments [9,10]. PTFE and titanium are not resorbable, and this requires a second surgical intervention after the bone [11–14] and may increase the rate of post-operatory complications [9]. On the other hand, collagen has low mechanical properties and irregular degradation, which impairs the space maintenance ability over time [8,15]. Several synthetic polymers have been studied to this end. Still, they mostly lack adequate handling, and none of these materials presents bioactive properties to contribute to bone formation in the defect site, requiring the combination of granular bone grafts to enhance bone repair [16–19]. Due to these differences, the clinical application of GBR membranes varies, and none of these materials fills the requirements for broad application in different clinical

situations [10]. The combination of adequate mechanical properties for space-maintaining capacity and handling should be combined with occlusive functions to avoid cell infiltration and, ideally, with bioactivity to contribute to cell activity and bone repair [10,20,21].

The design of novel GBR membranes may address these requirements in the combination of resorbable polymers with bioactive components for tailored mechanical and biological properties [22–26]. Several studies attempt to produce bioactive composite membranes with widely used synthetic polyesters [27–30]. The polybutylene adipate terephthalate (PBAT) is a biodegradable aliphatic-aromatic polyester composed of adipic acid, 1,4-butanediol, and terephthalic acid. These two units are responsible for the low crystallization in these polymers [31] and high flexibility [32] of its polymeric chains, making PBAT a candidate GBR membrane's production with tailored mechanical properties. As a flexible polyester, PBAT allows incorporating inorganic particles into its structure without compromising its handling. In this case, the addition of bioactive particles such as bioactive glasses could be used to combine the space maintenance ability of the PBAT with the osteogenic potential of these particles [33,34]. The niobium-containing bioactive glasses (BAGNb) were studied in granule and scaffolds forme in previous studies showing the ability of these compounds to promote bone regeneration *in vitro* [35] and *in vivo* [36]. The presence of niobium is shown to enhance sol-gel-derived bioactive glasses' bioactivity and may be positive for GBR procedures. The production of PBAT/BAGNb membranes may be a strategy to combine bioactive properties with controlled mechanical behavior for GBR membranes. Thus, this study aimed to develop bioactive GBR membranes by manufacturing PBAT/BAGNb composites as casting films. The composites were

chemically characterized, and the membranes were analyzed for their physicomechanical and biological properties.

2. Materials and Method

2.1 BAGNb synthesis

The niobium-containing bioactive glasses were produced according to a previous study [35]. Briefly, the niobium chloride ($NbCl_5$ – CBMM Companhia Brasileira de Metalurgia e Mineração, Araxá, Minas Gerais, Brasil) was used as a niobium source and added to an acidic solution with tetraethylorthosilicate (Sigma-Aldrich, St. Louis, MO, USA) for the sol-gel synthesis. The triethylphosphate (Sigma-Aldrich, St. Louis, MO, USA), calcium nitrate ($Ca(NO_3)_2$; Química Moderna, Barueri, São Paulo, Brazil) and sodium nitrate ($NaNO_3$; Química Moderna, Barueri, São Paulo, Brazil) were used as modifiers as well. The gel was kept at room temperature for five days and submitted to heat treatment at 70ºC, 120ºC, and 700ºC for 24 hours. The obtained powder was grounded and sifted with mesh 80 sieves before the incorporation into the polymer. The resultant particles presented with an average particle size of 4.56µm and surface area of 3.17m^2/g.

2.2 Composite preparation

Hot-melt extrusion was used to produced composites with adequate dispersion of polymer and bioactive glass particles. Poly(butylene adipate-co-terephthalate) (PBAT- Ecoflex® F Blend C1200; BASF Corporation, Florham Park, NJ, USA) pellets with 1.27g/cm^3 at 23ºC density were used. Different concentrations of BAGNb were used in composite preparation: 10 wt%, 20 wt%,

and 30 wt% and pure PBAT (control). Composites were prepared by a hot-melt extrusion process using twin-screw extrusion (Haake H-25, Rheomex PTW 16/25- Polylabsystem, Karlsruhe, Germany) at 150rpm rotation. During the extrusion, the temperature profile was 120/130/130/135/140°C from the barrel section just after the feed throat to the die. The extrudate was cooled in water.

2.3. Composite characterization

2.3.1. Fourier-Transformed Infrared Spectroscopy

The chemical structure of composites was assessed via the Fourier-transformed infrared spectroscopy (FTIR) was used in a spectrometer (Vertex 70 - Bruker Optics, Ettlingen, Germany) equipped with an attenuated total reflectance device (Platinum ATR-QL; Bruker Optics). The composite solution was placed above the ATR device in mold (4mm diameter and 1mm height; n = 1) until solvent evaporation to ensure adequate contact between the materials and the ATR device. The analysis was performed in the 400-4000cm^{-1} in 16 scans for each sample.

2.3.2. Thermogravimetric Analysis

To assess the thermal behavior of developed composites, thermogravimetric analysis (TGA) was performed. A thermogravimetric analyzer (TGA Discovery – TA Instruments, New Castle, DE, USA) was used. The samples were weighed (0.5g ± 0.01), placed in a platinum pan, and heated up to 600ºC at a rate of 10°C. min^{-1} under nitrogen purge (25 mL. min^{-1}). The weight loss (%) after the heating process (TGA) and the differential thermogravimetric (DTG) were used to determine the thermal behavior and the derivative weight

loss, respectively. The analyses were performed in specimens immediately after preparation and after 7, 14, and 28 days of immersion in simulated body fluid (SBF), prepared according to a standard protocol [37].

2.4 Barrier membrane production

The composite extruded filaments were used to produce the membranes by solvent casting. Chloroform (Labsynth – Diadema, São Paulo, Brazil) was used as the solvent in 1:7.5 (v/w) proportion. The solution was poured into a glass slide and stored at 37ºC for 1h for the complete evaporation of the solvent. The produced membranes were cut to produce the specimens for each characterization test.

2.5 Membrane characterization

2.5.1 Mechanical Behavior

The mechanical behavior of developed barrier membranes was assessed by a tensile test with hourglass specimens that were prepared according to ASTM D638-02 [38] type IV plastics. After the specimen preparation, they were tested immediately and, after 28 days of immersion in SBF, prepared as described in section 2.4.3. The tensile strength analysis was performed. The specimens were submitted to the tensile strength test in a test machine (Shimadzu EZ-SX, Shimadzu Corp., Kyoto, Japan) at a 1mm/min cross-head speed. The ultimate tensile strength, the young's module, and the elongation rate were calculated from the obtained data.

2.5.2 Scanning Electron Microscopy

The scanning electron microscopy (SEM) analysis was performed to evaluate the morphology of the barrier membrane's surface. The samples (6mm diameter x 0.2mm height; n = 1) were placed on stubs with carbon tape and gold-coated for the analysis. An electron microscope (JEOL 6060) was used to acquire the images in 1000x magnification at 10kV.

2.5.3 Contact Angle

The contact angle was measured on the samples' surface by the sessile drop method using distilled water. Both the top and the bottom of the samples were analyzed. The samples (6mm diameter x 0,2mm height; n = 3) were placed on top of glass slides, and one drop of water was poured on top of the membraned in an optical tensiometer (Theta Line, Biolin Scientific, Stockholm, Sweden). A high-resolution camera monitored the water's behavior on the material surface, and measurements of the contact angle were performed after 10 seconds by an image software (OneAttension - Biolin Scientific, Stockholm, Sweden). Three measurements were made in each sample.

2.5.4 Profilometry

Optical profilometry measured the surface properties of the developed barrier membranes (Optical Profiler ContourGT – Bruker). The samples (6mm diameter x 0.2 mm height; n = 3) were fixed on glass slides and scanned with 5x monochromatic light by vertical scanning interferometry. Both the top and the bottom of the samples were analyzed. The depth of the analysis ranged between 20 and 2000 nm, and the scanned area was 1260 µm x 1260 µm. The Ra parameter was measured as the arithmetic average of the surface roughness profile in samples.

2.5.5 pH

For pH analysis a digital phmeter was used (DM-22. Digimed,Brazil). were immersed in deionized water for up to 28 days. Membranes samples (6mm diameter x 0.2mm height; n = 3) were immersed in deionized water as previously described [39]. Samples were maintained at 37ºC in between measurements.

2.6 Cell behavior

The cell behavior analysis was performed with preosteoblastic MC3T3-E1 cell line Banco de Células do Rio de Janeiro, Rio de Janeiro, Brazil) The MC3T3-E1 cells were cultivated with α-MEM supplemented with 10% fetal bovine serum and 1% penicillin (Thermo Fischer Scientific, Waltham, Massachusets, EUA) at 37ºC at 5% CO_2.

2.6.1 Cell Proliferation

The cell proliferation was assessed by the sulphodhamine B (SRB) assay. Membrane specimens (6mm diameter x 0.2mm height; n = 3) were immersed in a culture medium for 24 hours prior to the analysis to produce a conditioned medium. The MC3T3-E1 cells were cultivated at $5x10^3$ density in a 96-well plate and treated with a conditioned medium for 72 hours. Wells, without conditioned medium, was cultivated and used as control. After treatment, cells were fixed and stained with 0.4% SRB solution. The amount of SRB dye was quantified at 560nm in a Microplate Spectrophotometer (Multiskan GO, Thermo Fisher Scientific, Waltham, Massachusets, USA). The results were normalized for the absorbance in wells without the conditioned medium.

2.6.2 Cell Mineralization

Cell mineralization was evaluated by the Alizarin S Red staining. Membrane specimens (12mm diameter x 0.2mm height; n = 3) were immersed in a culture medium for 24 hours prior to the analysis to produce a conditioned medium. Medium without membranes was used as well. The MC3T3-E1 were cultivated in osteogenic medium supplemented with 0.0023 g/mL β-glycerophosphate, and 0.05 mg/mL L-ascorbate at 2 x 10^4 density in 24 well-plates. The cell treatment was performed during 7, 14, and 21 days. After each time point, the wells were washed with PBS and stained with 2% Alizarin S Red solution (Sigma Aldrich, St, Louis, E.U.A.) for 20 minutes. Images were taken with a camera with 5x magnification and were analyzed in an image software (ImageJ National Institutes of Health, Bethesda, MD, USA). The % of the mineralized area in each well was calculated considering the measurement of the thresholded red intensity area. The same threshold was used for all images. The % of mineralized nodules in each well was normalized for the values found in wells treated with pure DMEM.

2.7 Statistical Analysis

Descriptive analysis was performed for the FTIR, SEM, TGA, profilometry, and HE analysis. The normality of data was tested with Shapiro-Wilk. One-way analysis of variance (ANOVA) and Tukey were used to cell proliferation data analysis. Two-way ANOVA was used for contact angle, pH, surface roughness, ultimate tensile strength, young's module, elongation at break, and cell mineralization.

3. Results

Figure 1 shows the results for the characterization of developed composites by FTIR and TGA. In FTIR analysis (Figure 1A) the PBAT group showed characteristic C-O bonding at 1105 cm^{-1} and 1270 cm^{-1} and C=O bonding at 720 cm^{-1} and 1710 cm^{-1}. These structures were found in groups with BAGNb addition that presented Si-O-Si bonding at 450 cm^{-1} and 1050 cm^{-1}. Pure PBAT presented a single stage of thermal degradation between 370ºC and 420ºC (Figure 1B). In this case, more than 90% of the weight was lost in a single stage, with a rate of weight loss that reached 2.46% at 400ºC (Figure 1C). This profile was not modified for the pure PBAT over time (Figure 1B and 1C). The immediate analysis shows that the addition of BAGNb affected the thermal degradation of composites decreasing the maximum degradation temperature at ~310ºC (Figure 1B).

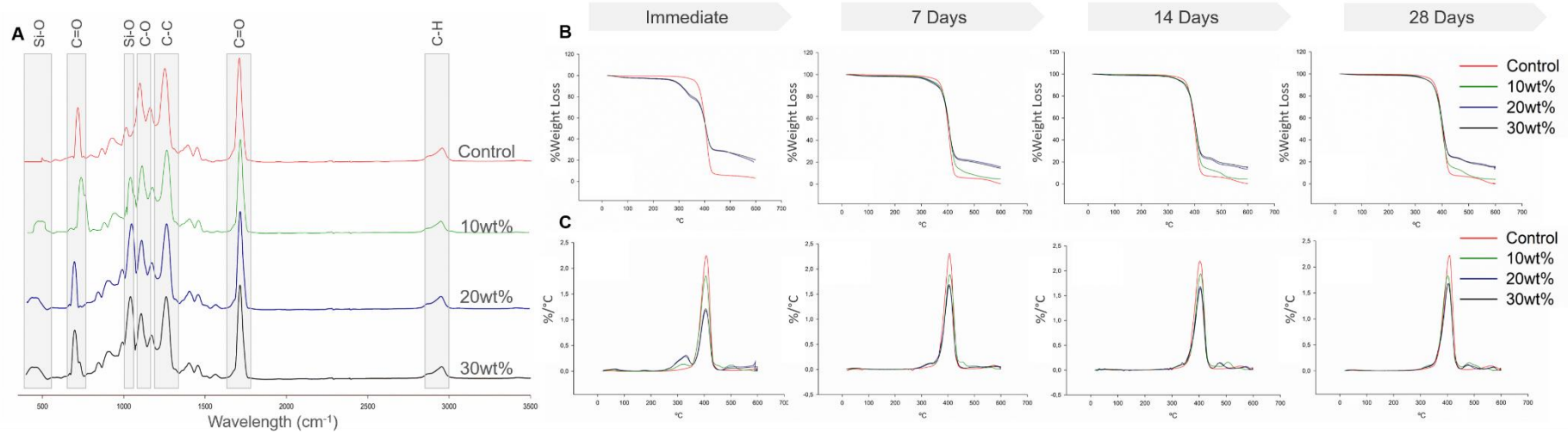

Figure 1. Composite Characterization. (A) FTIR analysis of developed composites with the chemical bonding found for each group and (B) TGA results with weight loss after heating in an immediate analysis and up to 28 days of immersion in SBF. (C) DTG curves showing the rate of weight loss before and after immersion in SBF, showing differences in thermal behavior between pure PBAT and the developed composites.

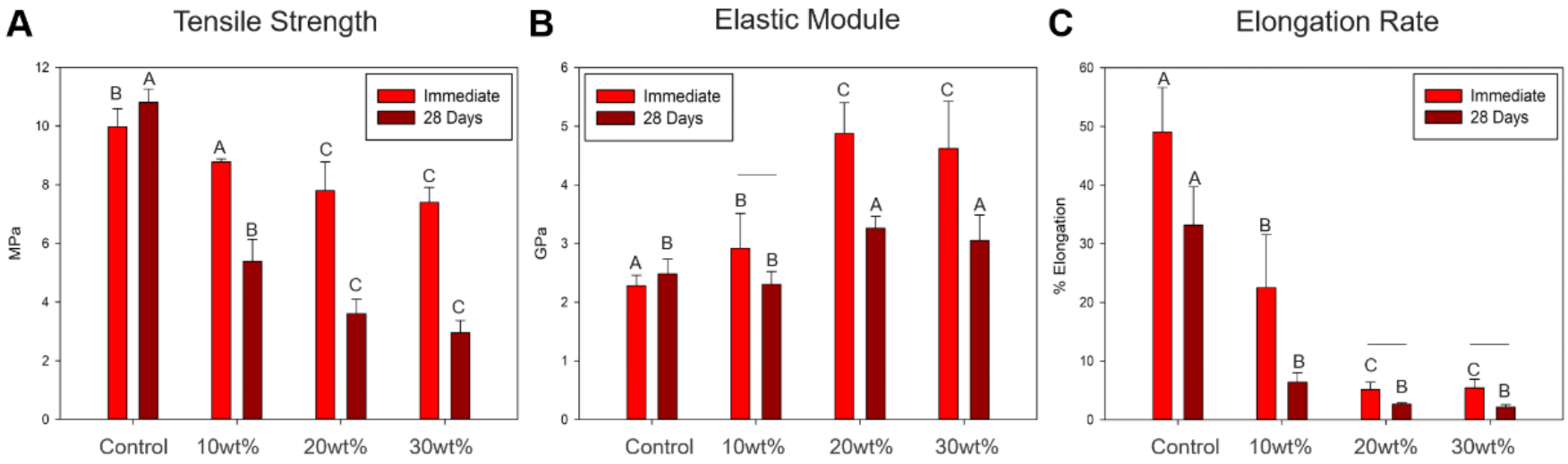

Figure 2. Mechanical behavior of developed barrier membranes. The tensile test was used to assess the tensile strength (MPa), Young's module, and the elongation rate in dry as prepared membranes and after 28 days of immersion in SBF.

The mechanical behavior of developed barrier membranes is shown in Figure 2. The addition of BAGNb at 20wt% and 30wt% concentration reduced the barrier membrane tensile strength both in immediate analysis and after their degradation (Figure 2A). These two values were affected by the immersion in SBF, where lower GPa values were found for Young's module, and the elongation rate reached 2.65% and 2.16% for 20wt% and 30wt%, respectively. The 20wt% and 30wt% membranes presented higher immediate stiffness in the immediate analysis associated with a lower elongation rate, as shown in Figure 2C.

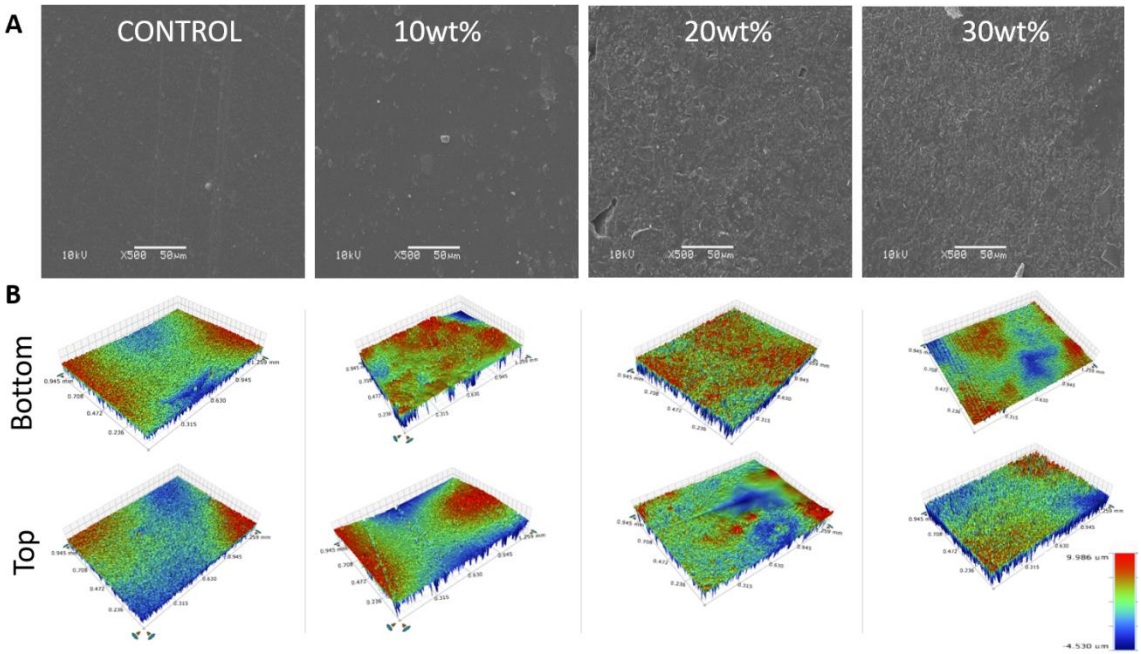

C

	Control		10wt%		20wt%		30wt%	
	Bottom	Top	Bottom	Top	Bottom	Top	Bottom	Top
Contact Angle (θ)	65.39 (±6.80)^{aA}	66.70 (±4.24)^{aA}	67.17 (±7.23)^{aA}	67.23 (±1.12)^{aA}	22.52 (±6.93)^{aB}	56.04 (±10.82)^{bA}	34.45 (±8.31)^{aB}	63.62 (±5.87)^{Ba}
Surface Roughness (μm)	0.54 (±0.08)^{aB}	0.66 (±0.15)^{aA}	1.04 (±0.38)^{aAB}	0.53 (±0.11)^{aA}	0.97 (± 0.42)^{aAB}	0.76 (±0.03)^{abA}	1.43 (±0.59)^{bB}	0.74 (±0.10)^{aA}

Different uppercase letters indicate a statistically significant difference between groups on each side of the membrane. Different lowercase letters indicate statistically significant difference between the side of membranes in each group.

Figure 3. Barrier membrane surface characterization. (A) The SEM analysis of the top surface. (B) Representative images of profilometry analysis at the bottom and the surface of the membranes and (C) Contact angle (θ) and surface roughness (μm) results of the bottom and top surfaces of developed membranes.

The SEM analysis is shown in Figure 3B. The barrier membrane's surface was shown with a smooth surface for the PBAT group, while the addition of BAGNb promoted an increase in the samples' roughness. Representative images of profilometry analysis show different color intensities along the membranes (Figure 3B). The red areas represent higher peaks on the membranes' surface, and green/blue areas represent reduced values. The contact angle shows statistically significant lower values for 20wt% and 30wt% groups on the membranes' bottom side, while no statistically significant difference was found on top (Figure 3C). The bottom side of membranes with 20wt% and 30wt% addition of BAGNb presented reduced contact angle values when compared to the top. The surface roughness values on the top surface presented no statistical difference between groups, while the bottom surface presented reduced values for the 20wt% and 30wt% groups (Figure 3C).

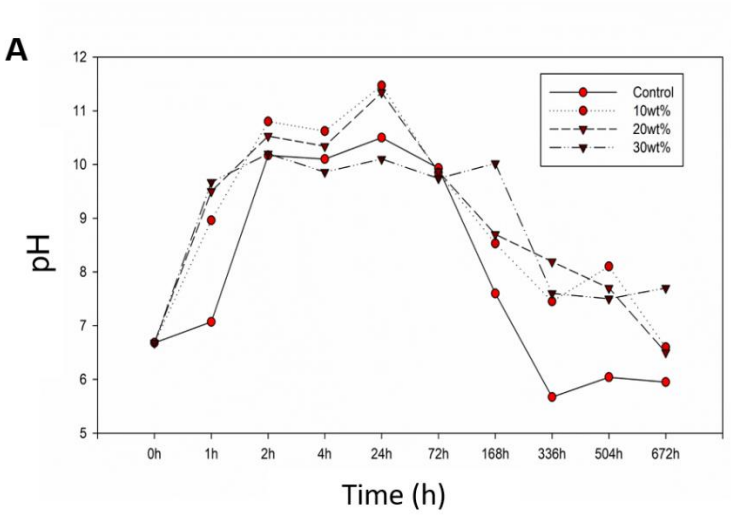

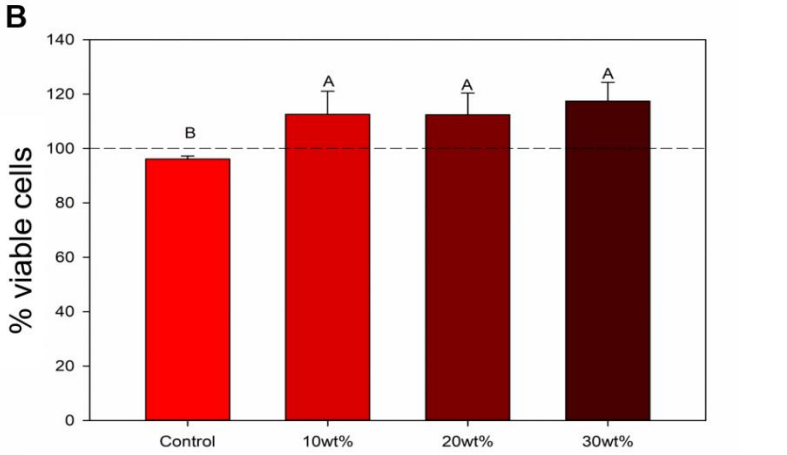

Different uppercase letters indicate statistically significantly difference between groups.

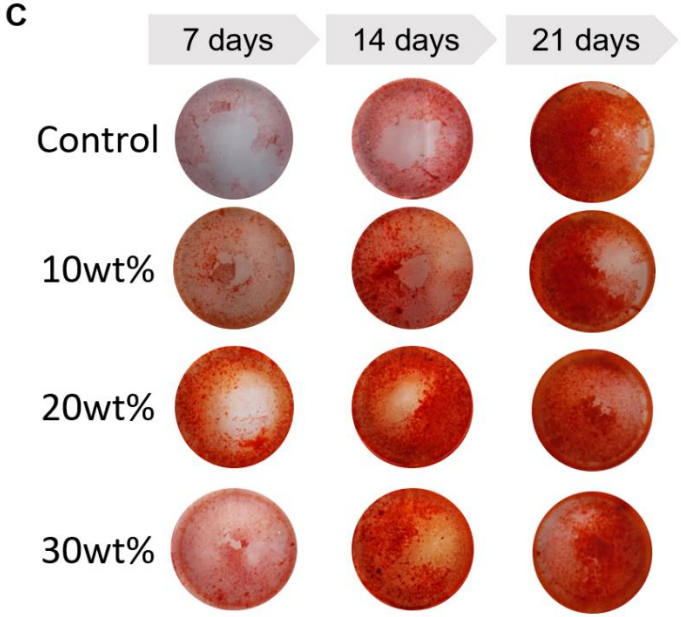

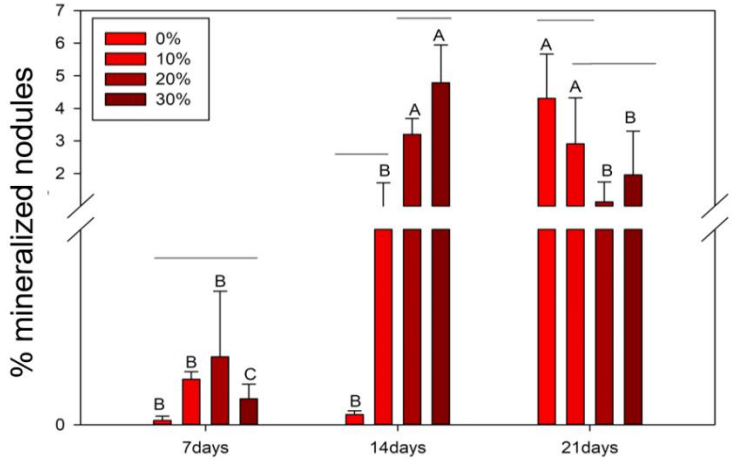

Different uppercase letters indicate statistically significantly difference between groups. Connected segments shows no statistically significant difference between time points.

Figure 4. pH, cell viability, and mineralization results. (A) Increased pH was observed for all groups in water and maintained higher for BAGNb containing membranes up to 28 days. (B) cell viability was higher for barrier membranes with the addition of BAGNb, regardless of the concentration used. (C) representative images for alizarin s red staining after 7, 14, and 21 days. (D) mineralization was quantified, and increased values were found for 20wt% and 30wt% after 14 days.

The immersion of barrier membrane specimens into water leads to an increase in pH values. A sharp increase was observed on the BAGNb-containing membranes, while environment modifications took place only after 2h for the control group. Barrier membranes with 10wt% and 20wt% reached 11.47 and 11.34 after 24h, respectively. The viability of MC3T3-E1 cells is shown in Figure 4B. Increased percentage values were found for barrier membranes with BAGNb ($p < 0.05$). Representative alizarin s red mineralization results show the differences in mineralization in different groups and culture times (Figure 4C). The % of the area covered by mineralized granules is observed in Figure 4D. Increased mineralization was observed for 20wt% and 30wt% groups after 14 days. In the 21-day analysis, higher calcium deposits were observed for 10wt% and for the control group when compared to higher concentrations of BAGNb ($P < 0.05$).

4. Discussion

Guided bone regeneration is known as an effective approach for increasing bone regeneration for rehabilitation in craniofacial surgery [1,3,12,40]. Barrier membranes are used for keeping space for bone formation and preventing the infiltration of soft tissue, but they may also be used to contribute to the

formation of bone in the regeneration site [6,41]. In this study, bioactive composite membranes were produced with PBAT and BAGNb and were designed with adjusted stiffness and strength to facilitate their clinical performance and application. The developed composites presented chemical and mechanical stability, and the produced membranes were shown to present surface features and ion release that may contribute to the bone formation of the maintained space.

Melt-extrusion was used in this study to produce PBAT/BAGNb composites to guarantee the temperature-driven dispersion of inorganic components into the polymeric matrix. The composite characterization is shown in Figure 1A, where the maintenance of PBAT structure was observed even with 30wt% of BAGNb. The maintenance of PBAT chemical structure was desired in the composites' design as the flexibility of PBAT could contribute to the handling in the application of the membranes in surgical sites as the random copolymerized structure is preserved [31]. The C-O-C bonding at 1160cm^{-1} and 1270cm^{-1} that are observed in Figure 1 A are assigned to the aliphatic and aromatic esters, respectively [31]. Although the aromatic unit is prone to crystallization, all aliphatic portions present an amorphous structure [42]. The molecule organization maintains the deformation ability of PBAT, which is not usually observed in other bioresorbable polymers with higher crystallinity [28,43]. The addition of BAGNb in the melt-extrusion process did not modify the backbone structure of PBAT and promoted differences in the thermal behavior of developed composites, as seen in Figure 1B. The immediate analysis showed that an additional weight loss was found in BAGNb-containing membranes that may be related to the condensation of remaining silanol groups in the glasses (Figure 1B)

[44]. This was not observed over time in the TGA analysis as these structures may be lost upon immersion. The DTG peaks may present important insights about the effect of BAGNb in the thermal degradation of developed composites (Figure 1C). In all groups, the maximum decomposition is found at ~420ºC where the ester bonding is broken (Figure 1C), but in BAGNb-containing groups, additional decomposition is observed. For the immediate analysis, the silanol decomposition is assigned to the peak at ~300ºC while the analysis after the immersion in SBF show a decomposition around 500ºC that may be related to the crystallization of hydroxyapatite, indicating that the immersion in SBF promoted the deposition of calcium phosphates in the membrane structure [45]. The degradation pattern found here is comparable to other studies' observations, showing that little effect of BAGNb is found [28,46,47]. The bioresorbability of barrier membranes is of major importance as non-resorbable membranes, such as the titanium ones, require additional interventions for their removal, increasing the need for surgical procedures and patients' morbidity [9,48]. The effect of degradation may be immediately observed on the pH and cell bevavior results (Figure 4) due to BAGNb ion release and may be further addressed to understand the immune response in the future analysis [15,19,49]

The handling of commercially available barrier membranes presents wide variations [24]. Among the non-resorbable membranes, stiff titanium mashes are used as space maintainers. Their increased stiffness is known to favor lesions in the soft tissue, leading to membrane exposure and failure [9]. On the other hand, collagen resorbable membranes are soft materials with low resistance that may impair the space maintaining ability [50–52]. Several synthetic bioresorbable polymers, such as PLA, PCL, and PLGA have been used to balance resistance

and stiffness [17,18,53–55]. However, the addition of bioactive inorganic particles to these polymers leads to a significant increase in stiffness, and the resultant composites present high elastic module values [17,18,53–55]. The modifications in the polymeric structure after the addition of inorganic particles may impair the handling, making difficult their adaptation in different surgical site configurations and may lead to clinical drawbacks like the dehiscence of soft tissue [10,24]. In this sense, PBAT flexibility could be used to control the stiffness in these composites, even at high concentrations of bioactive inorganic particles (Figure 2). Although a reduction in resistance and an increase in stiffness is observed as the BAGNb concentration increases, the obtained values are comparable to particle-free synthetic polymers [17,54].

An irregular surface is observed on the bottom of 20wt% and 30wt% BAGNb membranes, as shown in SEM (Figure 3A) and profilometry (Figure 3B) analysis and confirmed by contact angle (Figure 3C). By the membrane preparation, it was observed that the bottom surface presented increased roughness that was combined with a lower contact angle. This may be assigned to the combination of high hydrophilicity of BAGNb [56] and the obtained rough structure caused by particles, which could be mostly observed on the 30wt% group that achieved 34.45º at the contact angle analysis (Figure 3C). As a copolyester, PBAT presents a hydrophobic surface [57,58], and lowering the contact angle may contribute to the interaction between the polar groups on the surface material and the wet environment promoted by the presence of blood during the surgical procedure. This could promote a better adjustment of the membrane into the bone defects promoting a higher interaction of the membrane with the blood cloth and the cells surrounding this area [57]. Although the bottom

portion could be used for better interaction between the bone defect and the bioactive ions from the niobium-containing bioactive glasses, the top surface has an advantage since it can be applied directly in contact with soft tissues to prevent adhesion. As the guided bone regeneration aims to avoid the proliferation of cells and vascular tissue into the bone defect, the reduced roughness and increased contact angle could avoid the adhesion and proliferation of these cells over the membrane preventing the penetration [7,24].

The ion release promoted by bioactive glasses is well described [59], and this behavior is responsible for their ability to induce bone regeneration [60]. In this particular case, niobium was used as an adjuvant ion to increase the nucleation of minerals, stimulating bone deposition. These glasses were previously studied *in vitro* [35] and *in vivo* [36] for their ability to enhance cell activity and tissue formation, respectively. Ion release was assessed by modifications of pH in the environment, showing that membranes with BAGNb are not only able to induce an increase in the pH due to ions exchange in the medium, but they were also able to maintain these increased values over time (Figure 4A). A drop in pH values is observed over time in all membranes and this was expected as ion release stabilizes over time leading to precipitation in the media [33,39]. The release may be responsible for cell viability results (Figure 4B). The membranes with BAGNb addition promoted cell proliferation regardless of the concentration used (Figure 4), showing that these materials could favor the number of osteoblastic cells available for regeneration in the site after the guided bone regeneration procedure. More than that, the BAGNb modified these cells' responses regarding their ability to deposit minerals (Figure 4C and 4D). The presence of BAGNb increased the pre-osteoblastic differentiation that is

observed by their ability to deposit calcium-containing mineralized structures, as shown in the representative images in Figure 4C. Increased % of the mineralized area was observed for 20wt% and 30wt% membranes after 14 days. At 21 days, increased values are observed for the control group, followed by the 10wt%, while higher concentrations had reduced mineralized area. This may be assigned to saturation in the cell media with increased BAGNb concentrations that could lead to the lower content of minerals. Besides, it is known that MC3T3-E1 is able to differentiate after 21 days in osteogenic media and promote mineralization [61], as observed in this study (Figure 4D). However, loading BAGNb particles into PBAT membranes was shown to promote a faster differentiation and mineralization in cells in contact with these material products both at 7 and 14 days of analysis. Within the in vitro analysis, it is possible to highlight the possible modulation of cell behavior by the developed materials, especially when 30wt%BAGNb was used. GBR depends on the cell-to-cell interaction in the surgical site, and the use of PBAT/BAGNb membranes may contribute to the complex events related to bone repair during osteogenesis [62]. Further analysis may elucidate the role of degradation products of PBAT/BAGNb on the cell microenvironment, including the immune response and modulatory mechanisms that may affect bone tissue formation over time [63–65].

The development of materials that contribute as an additional bioactive surface for bone regeneration, with and without bone substitute materials, may contribute to a faster bone regeneration procedure facilitating the further steps in an implanted-supported tooth rehabilitation. In the present study, a novel composition for resorbable barrier membranes is shown with tailored mechanical properties in combination with potential bioactivity for the regeneration of bone

defects and augmentation of surgical sites. This could be translated as materials that are easy to handle and adapt into surgical defects with a reduced probability of soft tissue lesions while it provides support in the cell/material interaction by bioactive ion release for bone repair on the basis of guided bone regeneration. This *in vitro* analysis shows PBAT/BAGNb composites were shown for the fist time as an alternative to the commercially available membranes to provide resorbable, easily applicable and bioactive membranes for regenerative treatments.

5. Conclusion

The incorporation of up to 30wt% of BAGNb into PBAT barrier membranes maintained adequate chemical-mechanical properties leading to the production of materials with tailored surface properties and bioactivity that may increase bone formation in guided bone regeneration procedures.

References

[1] H. Aludden, A. Mordenfeld, C. Dahlin, M. Hallman, T. Starch-Jensen, Histological and histomorphometrical outcome after lateral guided bone regeneration augmentation of the mandible with different ratios of deproteinized bovine bone mineral and autogenous bone. A preclinical in vivo study, Clinical Oral Implants Research. 31 (2020) 1025–1036. https://doi.org/10.1111/clr.13649.

[2] V. Chappuis, M.G. Araújo, D. Buser, Clinical relevance of dimensional bone and soft tissue alterations post-extraction in esthetic sites, Periodontol. 2000. 73 (2017) 73–83. https://doi.org/10.1111/prd.12167.

[3] B. Wessing, S. Lettner, W. Zechner, Guided Bone Regeneration with Collagen Membranes and Particulate Graft Materials: A Systematic Review and Meta-Analysis, Int J Oral Maxillofac Implants. 33 (2018) 87–100. https://doi.org/10.11607/jomi.5461.

[4] S. Shahdad, E. Gamble, J. Matani, L. Zhang, A. Gambôa, Randomized clinical trial comparing PEG-based synthetic to porcine-derived collagen membrane in the preservation of alveolar bone following tooth extraction in

anterior maxilla, Clinical Oral Implants Research. 31 (2020) 1010–1024. https://doi.org/10.1111/clr.13648.

[5] S. Nyman, T. Karring, Regeneration of surgically removed buccal alveolar bone in dogs, Journal of Periodontal Research. 14 (1979) 86–92. https://doi.org/10.1111/j.1600-0765.1979.tb00221.x.

[6] D. Buser, L. Sennerby, H. De Bruyn, Modern implant dentistry based on osseointegration: 50 years of progress, current trends and open questions, Periodontology 2000. 73 (2017) 7–21. https://doi.org/10.1111/prd.12185.

[7] R. Gruber, B. Stadlinger, H. Terheyden, Cell-to-cell communication in guided bone regeneration: molecular and cellular mechanisms, Clinical Oral Implants Research. 28 (2017) 1139–1146. https://doi.org/10.1111/clr.12929.

[8] J. Becker, B. Al-Nawas, M.O. Klein, H. Schliephake, H. Terheyden, F. Schwarz, Use of a new cross-linked collagen membrane for the treatment of dehiscence-type defects at titanium implants: a prospective, randomized-controlled double-blinded clinical multicenter study, Clinical Oral Implants Research. 20 (2009) 742–749. https://doi.org/10.1111/j.1600-0501.2008.01689.x.

[9] J. Garcia, A. Dodge, P. Luepke, H.-L. Wang, Y. Kapila, G.-H. Lin, Effect of membrane exposure on guided bone regeneration: A systematic review and meta-analysis, Clinical Oral Implants Research. 29 (2018) 328–338. https://doi.org/10.1111/clr.13121.

[10] P. Aprile, D. Letourneur, T. Simon-Yarza, Membranes for Guided Bone Regeneration: A Road from Bench to Bedside, Advanced Healthcare Materials. 9 (2020) 2000707. https://doi.org/10.1002/adhm.202000707.

[11] G.E. Salvi, A. Monje, C. Tomasi, Long-term biological complications of dental implants placed either in pristine or in augmented sites: A systematic review and meta-analysis, Clinical Oral Implants Research. 29 (2018) 294–310. https://doi.org/10.1111/clr.13123.

[12] T. Basler, N. Naenni, D. Schneider, C.H.F. Hämmerle, R.E. Jung, D.S. Thoma, Randomized controlled clinical study assessing two membranes for guided bone regeneration of peri-implant bone defects: 3-year results, Clinical Oral Implants Research. 29 (2018) 499–507. https://doi.org/10.1111/clr.13147.

[13] A. Cucchi, M. Sartori, A. Parrilli, N.N. Aldini, E. Vignudelli, G. Corinaldesi, Histological and histomorphometric analysis of bone tissue after guided bone regeneration with non-resorbable membranes vs resorbable membranes and titanium mesh, Clinical Implant Dentistry and Related Research. 21 (2019) 693–701. https://doi.org/10.1111/cid.12814.

[14] N. Zeng, A. van Leeuwen, H. Yuan, R.R.M. Bos, D.W. Grijpma, R. Kuijer, Evaluation of novel resorbable membranes for bone augmentation in a rat model, Clinical Oral Implants Research. 27 (2016) e8–e14. https://doi.org/10.1111/clr.12519.

[15] E. Calciolari, F. Ravanetti, A. Strange, N. Mardas, L. Bozec, A. Cacchioli, N. Kostomitsopoulos, N. Donos, Degradation pattern of a porcine collagen membrane in an in vivo model of guided bone regeneration, J. Periodont. Res. 53 (2018) 430–439. https://doi.org/10.1111/jre.12530.

[16] S. Shankar, L.-F. Wang, J.-W. Rhim, Incorporation of zinc oxide nanoparticles improved the mechanical, water vapor barrier, UV-light barrier, and antibacterial properties of PLA-based nanocomposite films, Mater Sci Eng C Mater Biol Appl. 93 (2018) 289–298. https://doi.org/10.1016/j.msec.2018.08.002.

[17] A.G.B. Castro, M. Diba, M. Kersten, J.A. Jansen, J.J.J.P. van den Beucken, F. Yang, Development of a PCL-silica nanoparticles composite membrane for Guided Bone Regeneration, Mater Sci Eng C Mater Biol Appl. 85 (2018) 154–161. https://doi.org/10.1016/j.msec.2017.12.023.

[18] Z. Hy, J. Hb, K. Je, Z. S, K. Km, K. Js, Bioresorbable magnesium-reinforced PLA membrane for guided bone/tissue regeneration, Journal of the Mechanical Behavior of Biomedical Materials. 112 (2020). https://doi.org/10.1016/j.jmbbm.2020.104061.

[19] de M. Nk, M. Ef, O. Rlms, de B.S. Iaw, M. Jpb, E. E, A. Ss, de V. Lmr, P. Fr, de S.T. E, Synergistic effect of adding bioglass and carbon nanotubes on poly (lactic acid) porous membranes for guided bone regeneration, Materials Science & Engineering. C, Materials for Biological Applications. 117 (2020). https://doi.org/10.1016/j.msec.2020.111327.

[20] L. Sbricoli, R. Guazzo, M. Annunziata, L. Gobbato, E. Bressan, L. Nastri, Selection of Collagen Membranes for Bone Regeneration: A Literature Review, Materials (Basel). 13 (2020). https://doi.org/10.3390/ma13030786.

[21] F. Briguglio, D. Falcomatà, S. Marconcini, L. Fiorillo, R. Briguglio, D. Farronato, The Use of Titanium Mesh in Guided Bone Regeneration: A Systematic Review, Int J Dent. 2019 (2019) 9065423. https://doi.org/10.1155/2019/9065423.

[22] W. Xiao, C. Hu, C. Chu, Y. Man, Autogenous Dentin Shell Grafts Versus Bone Shell Grafts for Alveolar Ridge Reconstruction: A Novel Technique with Preliminary Results of a Prospective Clinical Study, Int J Periodontics Restorative Dent. 39 (2019) 885–893. https://doi.org/10.11607/prd.4344.

[23] V.J. Sunandhakumari, A.K. Vidhyadharan, A. Alim, D. Kumar, J. Ravindran, A. Krishna, M. Prasad, Fabrication and In Vitro Characterization of Bioactive Glass/Nano Hydroxyapatite Reinforced Electrospun Poly(ε-Caprolactone) Composite Membranes for Guided Tissue Regeneration, Bioengineering (Basel). 5 (2018). https://doi.org/10.3390/bioengineering5030054.

[24] Y.D. Rakhmatia, Y. Ayukawa, A. Furuhashi, K. Koyano, Current barrier membranes: titanium mesh and other membranes for guided bone regeneration

in dental applications, J Prosthodont Res. 57 (2013) 3–14. https://doi.org/10.1016/j.jpor.2012.12.001.

[25] J. Caballe-Serrano, A. Munar-Frau, O. Ortiz-Puigpelat, D. Soto-Penaloza, M. Penarrocha, F. Hernandez-Alfaro, On the search of the ideal barrier membrane for guided bone regeneration, J Clin Exp Dent. (2018) 0–0. https://doi.org/10.4317/jced.54767.

[26] M. Toledano-Osorio, F.J. Manzano-Moreno, C. Ruiz, M. Toledano, R. Osorio, Testing active membranes for bone regeneration: A review, Journal of Dentistry. 105 (2021) 103580. https://doi.org/10.1016/j.jdent.2021.103580.

[27] K. Fukushima, M.-H. Wu, S. Bocchini, A. Rasyida, M.-C. Yang, PBAT based nanocomposites for medical and industrial applications, Mater Sci Eng C Mater Biol Appl. 32 (2012) 1331–1351. https://doi.org/10.1016/j.msec.2012.04.005.

[28] K. Fukushima, A. Rasyida, M.-C. Yang, Characterization, degradation and biocompatibility of PBAT based nanocomposites, Applied Clay Science. 80–81 (2013) 291–298. https://doi.org/10.1016/j.clay.2013.04.015.

[29] Y. Ren, J. Hu, M. Yang, Y. Weng, Biodegradation Behavior of Poly (Lactic Acid) (PLA), Poly (Butylene Adipate-Co-Terephthalate) (PBAT), and Their Blends Under Digested Sludge Conditions, J Polym Environ. 27 (2019) 2784–2792. https://doi.org/10.1007/s10924-019-01563-3.

[30] D. Zhao, T. Zhu, J. Li, L. Cui, Z. Zhang, X. Zhuang, J. Ding, Poly(lactic-co-glycolic acid)-based composite bone-substitute materials, Bioactive Materials. 6 (2021) 346–360. https://doi.org/10.1016/j.bioactmat.2020.08.016.

[31] A. Arslan, S. Çakmak, A. Cengiz, M. Gümüşderelioğlu, Poly(butylene adipate-co-terephthalate) scaffolds: processing, structural characteristics and cellular responses, Journal of Biomaterials Science, Polymer Edition. 27 (2016) 1841–1859. https://doi.org/10.1080/09205063.2016.1239945.

[32] S. Kashani Rahimi, R. Aeinehvand, K. Kim, J.U. Otaigbe, Structure and Biocompatibility of Bioabsorbable Nanocomposites of Aliphatic-Aromatic Copolyester and Cellulose Nanocrystals, Biomacromolecules. 18 (2017) 2179–2194. https://doi.org/10.1021/acs.biomac.7b00578.

[33] J.R. Jones, Reprint of: Review of bioactive glass: From Hench to hybrids, Acta Biomaterialia. 23, Supplement (2015) S53–S82. https://doi.org/10.1016/j.actbio.2015.07.019.

[34] W. Wang, K.W.K. Yeung, Bone grafts and biomaterials substitutes for bone defect repair: A review, Bioactive Materials. 2 (2017) 224–247. https://doi.org/10.1016/j.bioactmat.2017.05.007.

[35] G. de S. Balbinot, F.M. Collares, F. Visioli, P.B.F. Soares, A.S. Takimi, S.M.W. Samuel, V.C.B. Leitune, Niobium addition to sol-gel derived bioactive glass powders and scaffolds: In vitro characterization and effect on pre-

osteoblastic cell behavior, Dent Mater. (2018). https://doi.org/10.1016/j.dental.2018.06.014.

[36] G. de S. Balbinot, V.C.B. Leitune, D. Ponzoni, F.M. Collares, Bone healing with niobium-containing bioactive glass composition in rat femur model: A micro-CT study, Dent Mater. 35 (2019) 1490–1497. https://doi.org/10.1016/j.dental.2019.07.012.

[37] T. Kokubo, H. Takadama, How useful is SBF in predicting in vivo bone bioactivity?, Biomaterials. 27 (2006) 2907–2915. https://doi.org/10.1016/j.biomaterials.2006.01.017.

[38] D20 Committee, Test Method for Tensile Properties of Plastics, ASTM International, n.d. https://doi.org/10.1520/D0638-02.

[39] N. Stone-Weiss, E.M. Pierce, R.E. Youngman, O. Gulbiten, N.J. Smith, J. Du, A. Goel, Understanding the structural drivers governing glass–water interactions in borosilicate based model bioactive glasses, Acta Biomaterialia. 65 (2018) 436–449. https://doi.org/10.1016/j.actbio.2017.11.006.

[40] Y. Liang, X. Luan, X. Liu, Recent advances in periodontal regeneration: A biomaterial perspective, Bioactive Materials. 5 (2020) 297–308. https://doi.org/10.1016/j.bioactmat.2020.02.012.

[41] J. Wang, L. Wang, Z. Zhou, H. Lai, P. Xu, L. Liao, J. Wei, Biodegradable Polymer Membranes Applied in Guided Bone/Tissue Regeneration: A Review, Polymers (Basel). 8 (2016). https://doi.org/10.3390/polym8040115.

[42] X.Q. Shi, H. Ito, T. Kikutani, Characterization on mixed-crystal structure and properties of poly(butylene adipate-co-terephthalate) biodegradable fibers, Polymer. 46 (2005) 11442–11450. https://doi.org/10.1016/j.polymer.2005.10.065.

[43] Q. Dou, J. Cai, Investigation on Polylactide (PLA)/Poly(butylene adipate-co-terephthalate) (PBAT)/Bark Flour of Plane Tree (PF) Eco-Composites, Materials (Basel). 9 (2016). https://doi.org/10.3390/ma9050393.

[44] I. Cacciotti, M. Lombardi, A. Bianco, A. Ravaglioli, L. Montanaro, Sol–gel derived 45S5 bioglass: synthesis, microstructural evolution and thermal behaviour, J Mater Sci: Mater Med. 23 (2012) 1849–1866. https://doi.org/10.1007/s10856-012-4667-6.

[45] A.A. El Hadad, E. Peón, F.R. García-Galván, V. Barranco, J. Parra, A. Jiménez-Morales, J.C. Galván, Biocompatibility and Corrosion Protection Behaviour of Hydroxyapatite Sol-Gel-Derived Coatings on Ti6Al4V Alloy, Materials. 10 (2017) 94. https://doi.org/10.3390/ma10020094.

[46] M.A. Abdelwahab, S. Taylor, M. Misra, A.K. Mohanty, Thermo-mechanical characterization of bioblends from polylactide and poly(butylene adipate-co-terephthalate) and lignin, Macromolecular Materials and Engineering. 300 (2015) 299–311. https://doi.org/10.1002/mame.201400241.

[47] G. Zehetmeyer, S.M.M. Meira, J.M. Scheibel, R.V.B. de Oliveira, A. Brandelli, R.M.D. Soares, Influence of melt processing on biodegradable nisin-PBAT films intended for active food packaging applications, Journal of Applied Polymer Science. 133 (2016). https://doi.org/10.1002/app.43212.

[48] W. Zhang, P. Li, G. Shen, X. Mo, C. Zhou, D. Alexander, F. Rupp, J. Geis-Gerstorfer, H. Zhang, G. Wan, Appropriately adapted properties of hot-extruded Zn–0.5Cu–xFe alloys aimed for biodegradable guided bone regeneration membrane application, Bioactive Materials. 6 (2021) 975–989. https://doi.org/10.1016/j.bioactmat.2020.09.019.

[49] C. Chu, J. Deng, X. Sun, Y. Qu, Y. Man, Collagen Membrane and Immune Response in Guided Bone Regeneration: Recent Progress and Perspectives, Tissue Eng Part B Rev. 23 (2017) 421–435. https://doi.org/10.1089/ten.TEB.2016.0463.

[50] P. Raz, T. Brosh, G. Ronen, H. Tal, Tensile Properties of Three Selected Collagen Membranes, BioMed Research International. 2019 (2019). https://doi.org/10.1155/2019/5163603.

[51] P. Chia-Lai, A. Orlowska, S. Al-Maawi, A. Dias, Y. Zhang, X. Wang, N. Zender, R. Sader, C.J. Kirkpatrick, S. Ghanaati, Sugar-based collagen membrane cross-linking increases barrier capacity of membranes, Clin Oral Invest. 22 (2018) 1851–1863. https://doi.org/10.1007/s00784-017-2281-1.

[52] Y. Wang, Y. Hua, Q. Zhang, J. Yang, H. Li, Y. Li, M. Cao, Q. Cai, X. Yang, X. Zhang, C. Li, Using biomimetically mineralized collagen membranes with different surface stiffness to guide regeneration of bone defects, Journal of Tissue Engineering and Regenerative Medicine. 12 (2018) 1545–1555. https://doi.org/10.1002/term.2670.

[53] C. Del Gaudio, A. Bianco, M. Folin, S. Baiguera, M. Grigioni, Structural characterization and cell response evaluation of electrospun PCL membranes: micrometric versus submicrometric fibers, J Biomed Mater Res A. 89 (2009) 1028–1039. https://doi.org/10.1002/jbm.a.32048.

[54] I. Yoshimoto, J.-I. Sasaki, R. Tsuboi, S. Yamaguchi, H. Kitagawa, S. Imazato, Development of layered PLGA membranes for periodontal tissue regeneration, Dent Mater. 34 (2018) 538–550. https://doi.org/10.1016/j.dental.2017.12.011.

[55] C. Shuai, W. Yang, P. Feng, S. Peng, H. Pan, Accelerated degradation of HAP/PLLA bone scaffold by PGA blending facilitates bioactivity and osteoconductivity, Bioactive Materials. 6 (2021) 490–502. https://doi.org/10.1016/j.bioactmat.2020.09.001.

[56] E. Verné, O. Bretcanu, C. Balagna, C.L. Bianchi, M. Cannas, S. Gatti, C. Vitale-Brovarone, Early stage reactivity and in vitro behavior of silica-based bioactive glasses and glass-ceramics, J Mater Sci: Mater Med. 20 (2009) 75–87. https://doi.org/10.1007/s10856-008-3537-8.

[57] F.Z. Amiri, Z. Pashandi, N. Lotfibakhshaiesh, M.J.M. Parsa, H. Ghanbari, R. Faridi-Majidi, Cell attachment effects of collagen nanoparticles on crosslinked electrospun nanofibers:, The International Journal of Artificial Organs. (2020). https://doi.org/10.1177/0391398820947737.

[58] Polycaprolactone nanofiber coated with chitosan and Gamma oryzanol functionalized as a novel wound dressing for healing infected wounds, International Journal of Biological Macromolecules. 164 (2020) 2358–2369. https://doi.org/10.1016/j.ijbiomac.2020.08.079.

[59] A. Hoppe, N.S. Güldal, A.R. Boccaccini, A review of the biological response to ionic dissolution products from bioactive glasses and glass-ceramics, Biomaterials. 32 (2011) 2757–2774. https://doi.org/10.1016/j.biomaterials.2011.01.004.

[60] A.A. El-Rashidy, J.A. Roether, L. Harhaus, U. Kneser, A.R. Boccaccini, Regenerating bone with bioactive glass scaffolds: A review of in vivo studies in bone defect models, Acta Biomater. 62 (2017) 1–28. https://doi.org/10.1016/j.actbio.2017.08.030.

[61] E.M. Czekanska, M.J. Stoddart, R.G. Richards, J.S. Hayes, In search of an osteoblast cell model for in vitro research, Eur Cell Mater. 24 (2012) 1–17. https://doi.org/10.22203/ecm.v024a01.

[62] N. Reznikov, J. a. M. Steele, P. Fratzl, M.M. Stevens, A materials science vision of extracellular matrix mineralization, Nature Reviews Materials. 1 (2016) 1–14. https://doi.org/10.1038/natrevmats.2016.41.

[63] C. Chu, L. Liu, S. Rung, Y. Wang, Y. Ma, C. Hu, X. Zhao, Y. Man, Y. Qu, Modulation of foreign body reaction and macrophage phenotypes concerning microenvironment, J Biomed Mater Res A. 108 (2020) 127–135. https://doi.org/10.1002/jbm.a.36798.

[64] C. Chu, L. Liu, Y. Wang, R. Yang, C. Hu, S. Rung, Y. Man, Y. Qu, Evaluation of epigallocatechin-3-gallate (EGCG)-modified scaffold determines macrophage recruitment, Mater Sci Eng C Mater Biol Appl. 100 (2019) 505–513. https://doi.org/10.1016/j.msec.2019.03.007.

[65] A. Cheng, C.E. Vantucci, L. Krishnan, M.A. Ruehle, T. Kotanchek, L.B. Wood, K. Roy, R.E. Guldberg, Early systemic immune biomarkers predict bone regeneration after trauma, Proc Natl Acad Sci U S A. 118 (2021). https://doi.org/10.1073/pnas.2017889118.

4 CONSIDERAÇÕES FINAIS

Novos biomateriais são desenvolvidos diante das desvantagens e das lacunas deixadas pelas membranas disponíveis para regeneração óssea guiada. Enquanto membranas de colágeno apresentam taxa de degradação irregular, baixa resistência mecânica e difícil manipulação, membranas não reabsorvíveis, como de PTFE e de titânio, requerem intervenção cirúrgica adicional para sua remoção e podem aumentar a taxa de complicações pós-operatórias. Diferentes estratégias são utilizadas para produzir novas membranas com adequadas propriedades para impedir a proliferação de tecido epitelial e conjuntivo para o interior do defeito, conferir estabilidade à ferida cirúrgica e estimular a regeneração óssea. A produção de membranas compósitas permite a união de propriedades de diferentes materiais. O PBAT, um polímero biocompatível, reabsorvível, flexível e resistente confere uma matriz polimérica adequada para a aplicação como barreira. O vidro bioativo possui a capacidade de gerar respostas benéficas no organismo, estimulando o reparo ósseo a nível celular através do aumento da expressão de genes envolvidos no processo de ossificação. As metodologias empregadas neste estudo revelam que a incorporação de vidro bioativo ao PBAT resultou em uma membrana com adequada superfície, capaz de interagir com as células através da dissolução iônica e estimular sua proliferação, diferenciação e a produção de material mineralizado. O compósito também apresentou propriedades mecânicas satisfatórias, requisito importante para suportar o crescimento tecidual, evitar o colapso e facilitar o manuseio do material. Os resultados obtidos colaboram para a conclusão de que a membrana produzida tem potencial para ser empregada em procedimentos que utilizam os princípios da regeneração óssea guiada. Considera-se oportuno o avanço nos métodos de avaliação da membrana desenvolvida, como estudos em animais, para que novos dados sejam obtidos a respeito do comportamento do compósito e da sua interação com tecidos vivos.

REFERÊNCIAS

ALLO, B. A.; RIZKALLA, A. S.; MEQUANINT, K. Synthesis and electrospinning of ε-polycaprolactone-bioactive glass hybrid biomaterials via a sol-gel process. **Langmuir**, [*s. l.*], v. 26, n. 23, p. 18340–18348, 2010. Available at: https://doi.org/10.1021/la102845k

ALTMANN, A. S. P. *et al.* In vitro antibacterial and remineralizing effect of adhesive containing triazine and niobium pentoxide phosphate inverted glass. **Clinical Oral Investigations**, [*s. l.*], v. 21, n. 1, p. 93–103, 2017. Available at: https://doi.org/10.1007/s00784-016-1754-y

ARAÚJO, M. G.; LINDHE, J. Dimensional ridge alterations following tooth extraction. An experimental study in the dog. **Journal of Clinical Periodontology**, [*s. l.*], v. 32, n. 2, p. 212–218, 2005. Available at: https://doi.org/10.1111/j.1600-051X.2005.00642.x

ARSLAN, A. *et al.* Poly(butylene adipate-co-terephthalate) scaffolds: processing, structural characteristics and cellular responses. **Journal of Biomaterials Science, Polymer Edition**, [*s. l.*], v. 27, n. 18, p. 1841–1859, 2016. Available at: https://doi.org/10.1080/09205063.2016.1239945

ATEF, M. *et al.* Horizontal ridge augmentation using native collagen membrane vs titanium mesh in atrophic maxillary ridges: Randomized clinical trial. **Clinical Implant Dentistry and Related Research**, [*s. l.*], v. 22, n. 2, p. 156–166, 2020. Available at: https://doi.org/10.1111/cid.12892

AVILA-ORTIZ, G. *et al.* Efficacy of Alveolar Ridge Preservation: A Randomized Controlled Trial. **Journal of Dental Research**, [*s. l.*], v. 99, n. 4, p. 402–409, 2020. Available at: https://doi.org/10.1177/0022034520905660

AVILA-ORTIZ, Gustavo; CHAMBRONE, L.; VIGNOLETTI, F. Effect of alveolar ridge preservation interventions following tooth extraction: A systematic review and meta-analysis. **Journal of Clinical Periodontology**, [*s. l.*], v. 46, n. S21, p. 195–223, 2019. Available at: https://doi.org/10.1111/jcpe.13057

BALBINOT, G. de S. *et al.* Bone healing with niobium-containing bioactive glass composition in rat femur model: A micro-CT study. **Dental Materials**, [*s. l.*], v. 35, n. 10, p. 1490–1497, 2019. Available at: https://doi.org/10.1016/j.dental.2019.07.012

BALBINOT, G. de S. *et al.* Niobium addition to sol-gel derived bioactive glass powders and scaffolds: In vitro characterization and effect on pre-osteoblastic cell behavior. **Dental Materials**, [*s. l.*], v. 34, n. 10, p. 1449–1458, 2018. Available at: https://doi.org/10.1016/j.dental.2018.06.014

BALBINOT, G. de S. *et al.* Niobium containing bioactive glasses as remineralizing filler for adhesive resins. **Dental Materials**, [*s. l.*], v. 36, n. 2, p. 221–228, 2020. Available at: https://doi.org/10.1016/j.dental.2019.11.014

BUNYARATAVEJ, P.; WANG, H.-L. Collagen Membranes: A Review. **Journal of Periodontology**, [*s. l.*], v. 72, n. 2, p. 215–229, 2001. Available at: https://doi.org/10.1902/jop.2001.72.2.215

BYEON, J. H. *et al.* Enhanced attachment of human osteoblasts on NH3-treated poly(L-lactic acid) membranes for guided bone regeneration. **Journal of Nanoscience and Nanotechnology**, [*s. l.*], v. 13, n. 3, p. 1691–1695, 2013. Available at: https://doi.org/10.1166/jnn.2013.6960

CABALLÉ-SERRANO, J. *et al.* On the search of the ideal barrier membrane for guided bone regeneration. **Journal of Clinical and Experimental Dentistry**, [*s. l.*], v. 10, n. 5, p. e477–e483, 2018. Available at: https://doi.org/10.4317/jced.54767

CARDAROPOLI, G.; ARAÚJO, M.; LINDHE, J. Dynamics of bone tissue formation in tooth extraction sites: An experimental study in dogs. **Journal of Clinical Periodontology**, [*s. l.*], v. 30, n. 9, p. 809–818, 2003. Available at: https://doi.org/10.1034/j.1600-051X.2003.00366.x

CHA, J. K. *et al.* Alveolar ridge preservation in the posterior maxilla reduces vertical dimensional change: A randomized controlled clinical trial. **Clinical Oral Implants Research**, [*s. l.*], v. 30, n. 6, p. 515–523, 2019. Available at: https://doi.org/10.1111/clr.13436

CLEMENTINI, M. *et al.* The effect of immediate implant placement on alveolar ridge preservation compared to spontaneous healing after tooth extraction: Radiographic results of a randomized controlled clinical trial. **Journal of Clinical Periodontology**, [*s. l.*], v. 46, n. 7, p. 776–786, 2019. Available at: https://doi.org/10.1111/jcpe.13125

COUSO-QUEIRUGA, E. *et al.* Post-extraction dimensional changes: A systematic review and meta-analysis. **Journal of Clinical Periodontology**, [*s. l.*], v. 48, n. 1, p. 126–144, 2021. Available at: https://doi.org/10.1111/jcpe.13390

CUCCHI, A. *et al.* Histological and histomorphometric analysis of bone tissue after guided bone regeneration with non-resorbable membranes vs resorbable membranes and titanium mesh. **Clinical Implant Dentistry and Related Research**, [*s. l.*], v. 21, n. 4, p. 693–701, 2019. Available at: https://doi.org/10.1111/cid.12814

DSOUKI, N. A. *et al.* Cytotoxic, hematologic and histologic effects of niobium pentoxide in Swiss mice. **Journal of Materials Science: Materials in Medicine**, [*s. l.*], v. 25, n. 5, p. 1301–1305, 2014. Available at: https://doi.org/10.1007/s10856-014-5153-0

ELGALI, I. *et al.* Guided bone regeneration: materials and biological mechanisms revisited. **European Journal of Oral Sciences**, [*s. l.*], v. 125, n. 5, p. 315–337, 2017. Available at: https://doi.org/10.1111/eos.12364

FUKUSHIMA, K. *et al.* PBAT based nanocomposites for medical and industrial applications. **Materials Science and Engineering C**, [*s. l.*], v. 32, n. 6, p. 1331–1351, 2012. Available at: https://doi.org/10.1016/j.msec.2012.04.005

GU, Y. *et al.* Biodegradable borosilicate bioactive glass scaffolds with a trabecular microstructure for bone repair. **Materials Science and Engineering C**, [*s. l.*], v. 36, n. 1, p. 294–300, 2014. Available at: https://doi.org/10.1016/j.msec.2013.12.023

HAGHIGHAT, A. *et al.* Histologic, Histomorphometric, and Osteogenesis Comparative Study of a Novel Fabricated Nanocomposite Membrane Versus Cytoplast Membrane. **Journal of Oral and Maxillofacial Surgery**, [*s. l.*], v. 77, n. 10, p. 2027–2039, 2019. Available at: https://doi.org/10.1016/j.joms.2019.05.012

HENCH, L. L. The story of Bioglass®. **Journal of Materials Science: Materials in Medicine**, [*s. l.*], v. 17, n. 11, p. 967–978, 2006. Available at: https://doi.org/10.1007/s10856-006-0432-z

JONES, J. R. Reprint of: Review of bioactive glass: From Hench to hybrids. **Acta Biomaterialia**, [*s. l.*], v. 23, n. S, p. S53–S82, 2015. Available at: https://doi.org/10.1016/j.actbio.2015.07.019

LEITUNE, V. C. B. *et al.* Niobium pentoxide as a novel filler for dental adhesive resin. **Journal of Dentistry**, [*s. l.*], v. 41, n. 2, p. 106–113, 2013. Available at: https://doi.org/10.1016/j.jdent.2012.04.022

LIN, Y. *et al.* Effect of copper-doped silicate 13-93 bioactive glass scaffolds on the response of MC3T3-E1 cells in vitro and on bone regeneration and angiogenesis in rat calvarial defects in vivo. **Materials Science and Engineering C**, [*s. l.*], v. 67, p. 440–452, 2016. Available at: https://doi.org/10.1016/j.msec.2016.05.073

MALLEGNI, N. *et al.* Poly(lactic acid) (PLA) based tear resistant and biodegradable flexible films by blown film extrusion. **Materials**, [*s. l.*], v. 11, n. 1, 2018. Available at: https://doi.org/10.3390/ma11010148

MENDOZA-AZPUR, G. *et al.* Horizontal ridge augmentation with guided bone regeneration using particulate xenogenic bone substitutes with or without autogenous block grafts: A randomized controlled trial. **Clinical Implant Dentistry and Related Research**, [*s. l.*], v. 21, n. 4, p. 521–530, 2019. Available at: https://doi.org/10.1111/cid.12740

MISAWA, M.; LINDHE, J.; ARAÚJO, M. G. The alveolar process following single-tooth extraction: a study of maxillary incisor and premolar sites in man. **Clinical Oral Implants Research**, [*s. l.*], v. 27, n. 7, p. 884–889, 2016. Available at: https://doi.org/10.1111/clr.12710

NAENNI, N. *et al.* Randomized clinical study assessing two membranes for guided bone regeneration of peri-implant bone defects: clinical and histological outcomes at 6 months. **Clinical Oral Implants Research**, [*s. l.*], v. 28, n. 10, p. 1309–1317, 2017. Available at: https://doi.org/10.1111/clr.12977

OH, S. A.; WON, J. E.; KIM, H. W. Composite membranes of poly(lactic acid) with zinc-added bioactive glass as a guiding matrix for osteogenic differentiation of bone marrow mesenchymal stem cells. **Journal of Biomaterials Applications**, [*s. l.*], v. 27, n. 4, p. 413–422, 2012. Available at: https://doi.org/10.1177/0885328211408944

PITALUGA, L. H. *et al.* Electrospun F18 bioactive glass/PCL-Poly (ε-caprolactone)-Membrane for guided tissue regeneration. **Materials**, [*s. l.*], v. 11, n. 3, 2018. Available at: https://doi.org/10.3390/ma11030400

RAKHMATIA, Y. D. *et al.* Current barrier membranes: Titanium mesh and other

membranes for guided bone regeneration in dental applications. **Journal of Prosthodontic Research**, [*s. l.*], v. 57, n. 1, p. 3–14, 2013. Available at: https://doi.org/10.1016/j.jpor.2012.12.001

RETZEPI, M.; DONOS, N. Guided Bone Regeneration: Biological principle and therapeutic applications. **Clinical Oral Implants Research**, [*s. l.*], v. 21, n. 6, p. 567–576, 2010. Available at: https://doi.org/10.1111/j.1600-0501.2010.01922.x

SU, H. *et al.* A comparison of two types of electrospun chitosan membranes and a collagen membrane in vivo. **Dental Materials**, [*s. l.*], v. 37, n. 1, p. 60–70, 2021. Available at: https://doi.org/10.1016/j.dental.2020.10.011

SUNANDHAKUMARI, V. J. *et al.* Fabrication and in vitro characterization of bioactive glass/nano hydroxyapatite reinforced electrospun poly(ε-caprolactone) composite membranes for guided tissue regeneration. **Bioengineering**, [*s. l.*], v. 5, n. 3, 2018. Available at: https://doi.org/10.3390/bioengineering5030054

TEMMERMAN, A. *et al.* Bovine-derived xenograft in combination with autogenous bone chips versus xenograft alone for the augmentation of bony dehiscences around oral implants: A randomized, controlled, split-mouth clinical trial. **Journal of Clinical Periodontology**, [*s. l.*], v. 47, n. 1, p. 110–119, 2020. Available at: https://doi.org/10.1111/jcpe.13209

TONETTI, M. S. *et al.* Management of the extraction socket and timing of implant placement: Consensus report and clinical recommendations of group 3 of the XV European Workshop in Periodontology. **Journal of Clinical Periodontology**, [*s. l.*], v. 46, n. S21, p. 183–194, 2019. Available at: https://doi.org/10.1111/jcpe.13131

VON ARX, T. *et al.* Membrane durability and tissue response of different bioresorbable barrier membranes: a histologic study in the rabbit calvarium. **The International journal of oral & maxillofacial implants**, [*s. l.*], v. 20, n. 6, p. 843–853, 2005. Available at: http://www.ncbi.nlm.nih.gov/pubmed/16392340

WEI, D. *et al.* Non-leaching antimicrobial biodegradable PBAT films through a facile and novel approach. **Materials Science and Engineering C**, [*s. l.*], v. 58, p. 986–991, 2016. Available at: https://doi.org/10.1016/j.msec.2015.09.023

XYNOS, I. D. *et al.* Ionic products of bioactive glass dissolution increase proliferation of human osteoblasts and induce insulin-like growth factor II mRNA expression and protein synthesis. **Biochemical and Biophysical Research Communications**, [*s. l.*], v. 276, n. 2, p. 461–465, 2000. Available at: https://doi.org/10.1006/bbrc.2000.3503

YOSHIMOTO, I. *et al.* Development of layered PLGA membranes for periodontal tissue regeneration. **Dental Materials**, [*s. l.*], v. 34, n. 3, p. 538–550, 2018. Available at: https://doi.org/10.1016/j.dental.2017.12.011

YUSOF, M. R. *et al.* Fabrication and characterization of carboxymethyl starch/poly(l-lactide) acid/β-tricalcium phosphate composite nanofibers via electrospinning. **Polymers**, [*s. l.*], v. 11, n. 9, 2019. Available at: https://doi.org/10.3390/polym11091468